



# Dynamic computed tomography evaluation of the nasopharynx in normal Beagle dogs

Daji NOH<sup>1)</sup>, Sooyoung CHOI<sup>2)</sup>, Hojung CHOI<sup>3)</sup>, Youngwon LEE<sup>3)</sup> and Kija LEE<sup>1)\*</sup><sup>1)</sup>College of Veterinary Medicine, Kyungpook National University, Daegu 41566, Korea<sup>2)</sup>College of Veterinary Medicine, Kangwon National University, Chuncheon 24341, Korea<sup>3)</sup>College of Veterinary Medicine, Chungnam National University, Daejeon 34134, Korea

**ABSTRACT.** Pharyngeal collapsibility has been used as diagnostic criteria in dogs, whereas the normal range and quantitative method have not been studied. Dynamic and static computed tomography (CT) was performed in 23 normal Beagle dogs to quantify the nasopharyngeal collapsibility at different locations. Using dynamic CT, maximum and minimum nasopharyngeal cross-sectional areas (CSAs) were measured at the level of the cranial end of the soft palate, pterygoid hamulus, foramen lacerum, bony labyrinth, and caudal end of the soft palate. The ratio of all maximum and minimum CSA to nasopharyngeal CSA at the level of the caudal hard palate (rCSAmax and rCSAmin) and the nasopharyngeal collapsibility were calculated. The differences of rCSAmax, rCSAmin, and nasopharyngeal collapsibility were analyzed at various locations. The nasopharyngeal collapsibility at the level of foramen lacerum, bony labyrinth, and caudal end of soft palate were higher than the others. At the level of the caudal end of the soft palate, rCSAmin was lower than that of the foramen lacerum and bony labyrinth, whereas rCSAmax at foramen lacerum was higher than that of the caudal end of the soft palate. These results indicated that the nasopharynx at the level of foramen lacerum and caudal end of the soft palate were considered notable locations for evaluating collapsibility. Dynamic CT could show the nasopharyngeal dynamic profile and will be an adequate modality for evaluating nasopharynx. Our results will be helpful for further comparative studies in dogs with and without nasopharyngeal collapse.

**KEY WORDS:** collapsibility, dog, dynamic computed tomography, nasopharynx

*J. Vet. Med. Sci.*

83(9): 1356–1362, 2021

doi: 10.1292/jvms.21-0216

Received: 9 April 2021

Accepted: 29 June 2021

Advanced Epub:

9 July 2021

Maintenance of the upper airway patency depends on a balance between forces dilating or collapsing the airway. These forces are composed of tissue stresses that act as radials through the airway and local airway pressure in the upper and thoracic airways [1]. During the respiratory cycle, local airway pressure changes, and affects the luminal area of the upper airway and the pharyngeal walls [6, 14, 19]. When an anatomic abnormality or pharyngeal dilator myopathy are present, the change of the luminal area in the upper airway is increased, causing a clinical pharyngeal collapse in humans [3, 9, 20]. For dogs, this is still unclear due to lack of studies [23, 24]. In small animal practice, pharyngeal collapse is anecdotally encountered on radiographs in both non-brachycephalic and brachycephalic dogs with and without stertor. In previous studies, the pharyngeal collapse is defined as complete when the pharynx loses the total air column, or partial air column when the luminal collapsibility is over the 50% in fluoroscopic study [23, 24]. However, there have been no studies focusing on a detailed quantification method for nasopharyngeal collapsibility and its normal range in dogs.

In veterinary medicine, computed tomography (CT) has been used in several studies of brachycephalic obstructive airway syndrome owing to its advantages in evaluating the entire upper respiratory system in detail and allowing reconstruction of original data into multiplanar and 3-dimensional images [10, 12, 18]. However, these studies used static CT, which has limitations because it does not reflect the dynamics of changes in the upper airway. In contrast, dynamic CT has the advantage of the feasibility of acquiring high-quality images that sufficiently delineate the upper airway contour and quantify the dynamic profile, as well as the advantages of static CT [9, 26, 28]. However, there have been very few dynamic CT studies of the upper airway in dogs [11].

In humans, there are differences in pharyngeal collapsibility by location, according to the presence or severity of obstructive sleep apnea [6, 13]. In dogs, a study in Pugs and French Bulldogs with obstructive airway syndrome showed that the smallest nasopharyngeal cross-sectional area (CSA) was located at the level of the caudal end of the soft palate [12]. However, the previous study evaluated the nasopharyngeal CSA using conventional CT and not by comparing the maximum and minimum cross-sectional area using dynamic CT. Thus far, there has been no study for nasopharyngeal collapsibility by location in dogs. Based

\*Correspondence to: Lee, K.: leekj@knu.ac.kr

(Supplementary material: refer to PMC <https://www.ncbi.nlm.nih.gov/pmc/journals/2350/>)

©2021 The Japanese Society of Veterinary Science



This is an open-access article distributed under the terms of the Creative Commons Attribution Non-Commercial No Derivatives (by-nc-nd) License. (CC-BY-NC-ND 4.0: <https://creativecommons.org/licenses/by-nc-nd/4.0/>)

on previous studies in humans that showed pharyngeal collapsibility in normal subjects and its variation by location [6, 13, 14, 19], we hypothesized that normal dogs have nasopharyngeal CSA change according to their respiratory cycle, and the degree of nasopharyngeal CSA change may differ depending on the location. Moreover, we hypothesized that nasopharyngeal collapsibility is correlated with adjacent structures, including soft palate and epiglottis. The study aimed to analyze nasopharyngeal collapsibility at various locations and to analyze its correlation with adjacent structures using static and dynamic CT in normal dogs. Consequently, our study aimed to determine the locations for evaluating nasopharyngeal collapsibility.

## MATERIALS AND METHODS

### Animals

A prospective and cross-sectional designed study was performed. Twenty-three male Beagle dogs were included in the study. The mean age was 5.0 years (1.8–5.5 years), and the mean body weight was 10.3 kg (8.0–13.3 kg). All procedures were in accordance with Kyungpook National University Animal Care and Use Committee guidelines (No. KNU 2020-0033). All dogs had a physical examination including cardiac and lung auscultation, and cervical tracheal manipulation to check the presence of coughing. Dogs with nasal discharge, sneezing, coughing, stertor, stridor, and retching were not included in this study. Before the CT scan, thoracic radiographs, a complete blood count, and a biochemical serum profile were performed. Ventrodorsal and right lateral thoracic radiographs were acquired in all dogs to identify the presence of lower airway collapse, cardiac disease, and pulmonary disease.

### Experimental protocol

Based on previous research showing that endotracheal intubation could change airway pressure [18], endotracheal intubation was not performed in this study. For sedation, 0.02 mg/kg medetomidine (Domitor; Pfizer, New York, NY, USA) was injected intravenously. The dog was positioned in sternal recumbency on the CT table. The head was held up using a sponge to maintain it in an extended neutral position with the hard palate parallel to the CT table. A self-manufactured bite block was placed between both canine teeth to maintain mouth opening for better visualization of upper airway structure [17]. The tongue was pulled out between the bite blocks. The respiratory rate was recorded after the respiratory rate fell to less than 20 breaths/min.

CT scans were performed using 32-Multislice CT (Alexion™; Canon Medical System, Otawara, Japan). The examination range included the rhinarium to the third cervical vertebra to evaluate the length and thickness of soft palate and to help choose the locations for dynamic CT. The CT scan parameters were as follows: 120 kV, 130 mA, 1.0 mm slice thickness, and 0.75 sec rotation times. All transverse images perpendicular to the hard palate and reconstructed sagittal images were obtained.

Transverse images were reviewed focused on the nasopharynx, and the following locations for the subsequent dynamic CT scans were chosen: (1) at the caudal hard palate (Fig. 1B); (2) at the cranial end of the soft palate, defined as the point where the torus

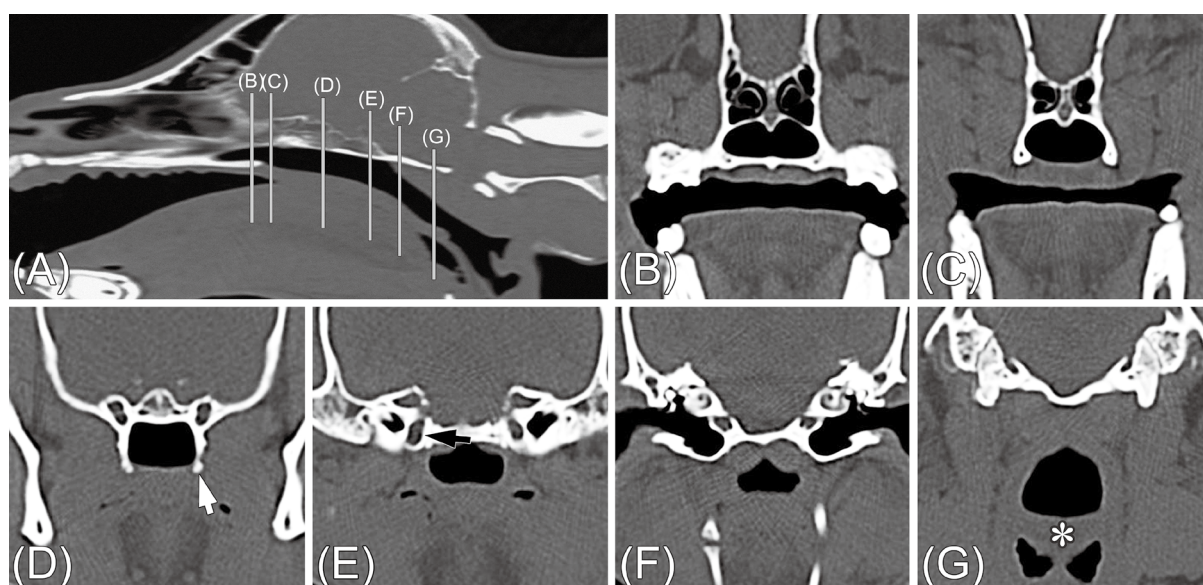


**Fig. 1.** The transverse CT images of the nasopharynx where dynamic CT scan was performed. Sagittal (A) and transverse nasopharyngeal images are shown in bone window setting (window width, 2700 HU, window level, 350 HU) at the level of the caudal hard palate (B), the cranial end of the soft palate (C), defined as the point where the torus palatinus discontinues, the pterygoid hamulus (D), defined as the point where the pterygoid hamulus extends most ventral (white arrow), the foramen lacerum (E), defined as the point where the widest canal of foramen lacerum (black arrow) is shown, the bony labyrinth (F), and the caudal end of the soft palate (G) where the caudal aspect of the intact soft palate (asterisk) is shown.

palatinus discontinues (Fig. 1C); (3) at the pterygoid hamulus, defined as the point where the pterygoid hamulus extends to most ventral (Fig. 1D); (4) at the foramen lacerum, defined as the point where the widest canal of foramen lacerum is shown (Fig. 1E); (5) at the bony labyrinth (Fig. 1F); and (6) at the caudal end of the soft palate, defined in front of the point where the soft palate diverges (Fig. 1G).

Dynamic CT scan was performed including at least two breathing cycles at 1-sec intervals. A field of view was used with the image being acquired in such a way as to place the nasopharynx in the center for each location. The dynamic CT images were obtained at the cranial end of the soft palate, pterygoid hamulus, foramen lacerum, bony labyrinth, and caudal end of the soft palate, respectively. After dynamic CT scan, 0.1 mg/kg atipamezole (Antisedan; Pfizer) was injected intramuscularly for sedation reversal and the condition was monitored until the dogs were able to stand on their own.

### CT data analysis

All CT imaging assessments and measurements were performed using a picture archiving and communication system (PACS) and its software (ZeTTA PACS Viewer; Taeyoung Soft, Seoul, Korea).

Using the mid-sagittal images of head and neck, the angle between hard palate and dorsal margin of the vertebral canal of axis was measured to verify the uniformity of CT scan positions. Based on the method in a previous study [9], soft palate length and thickness was measured at bone windows (window width, 2,700 HU; window level, 350 HU). The soft palate length was defined as the distance from the caudal margin of the hard palate to the tip of the soft palate. The soft palate thickness was defined as the thickest distance between the dorsal and ventral margin of the soft palate perpendicular to the soft palate length. On the transverse images of the head, nasopharyngeal CSA was measured at the level of the caudal hard palate. Regions of interest were drawn manually following the inner edge of the nasopharynx and were consequently calculated using the PACS software. In addition, the location of the epiglottis, whether it was below or above the soft palate, was recorded.

Using the dynamic CT images of the nasopharynx, maximum and minimum nasopharyngeal CSA were measured at bone windows at five locations: cranial end of the soft palate, pterygoid hamulus, foramen lacerum, bony labyrinth, and caudal end of the soft palate. For normalization, the ratio of all maximum and minimum CSAs at different locations to nasopharyngeal CSA at caudal hard palate (rCSAmax and rCSAmin) was calculated. The nasopharyngeal collapsibility was calculated at five locations: cranial end of the soft palate, pterygoid hamulus, foramen lacerum, bony labyrinth, and caudal end of the soft palate. Nasopharyngeal collapsibility was defined as the percentage of the difference between the maximum and minimum nasopharyngeal CSA, divided by the maximum nasopharyngeal CSA.

$$\text{Collapsibility (\%)} = \frac{\text{maximum CSA} - \text{minimum CSA}}{\text{maximum CSA}} \times 100$$

### Statistical analysis

All statistical analyses were performed using a commercial software program (SPSS 24.0; IBM SPSS statistics, Armonk, NY, USA). Shapiro–Wilk tests were used for the assessment of normality. According to distribution, Pearson or Spearman's correlation was used to evaluate the association of body weight with the dimensions of the soft palate and nasopharyngeal area variants, including maximum and minimum nasopharyngeal CSAs, rCSAmax, rCSAmin, and nasopharyngeal collapsibility at the cranial end of the soft palate, pterygoid hamulus, foramen lacerum, bony labyrinth, and caudal end of the soft palate. Moreover, the association between the dimensions of the soft palate and nasopharyngeal collapsibility was analyzed. Mann-Whitney *U* tests were used to ascertain the difference of nasopharyngeal collapsibility according to the epiglottis location.

To identify the differences in the nasopharynx at different locations, repeated ANOVA tests followed by *post hoc* Bonferroni test were performed in rCSAmax, rCSAmin, and nasopharyngeal collapsibility. *P*-values less than 0.05 were considered significant.

## RESULTS

The mean value  $\pm$  standard deviation (SD) of the angle between hard palate and dorsal margin of the vertebral canal of axis was  $172.9^\circ \pm 4.5^\circ$  (range,  $165.7^\circ$ – $178.7^\circ$ ). The mean values  $\pm$  SD for soft palate length and thickness were  $64.51 \pm 4.89$  mm and  $6.48 \pm 1.14$  mm, respectively. The mean values  $\pm$  SD for the dimensions of the soft palate, maximum and minimum nasopharyngeal CSA, rCSAmax, and rCSAmin are summarized in Tables 1 and 2. The median values with an interquartile range of nasopharyngeal collapsibility are summarized in Table 3.

There was significant positive correlation between soft palate thickness and body weight ( $r=0.574$ ,  $P<0.001$ , Table 1). Among the nasopharyngeal area variants, collapsibility at the bony labyrinth showed a positive correlation with body weight ( $r=0.499$ ,  $P<0.05$ , Table 3).

In the analysis of the correlation between the dimensions of the soft palate and nasopharyngeal collapsibility, collapsibility at the caudal end of the soft palate showed a negative correlation with soft palate length ( $r=-0.445$ ,  $P<0.05$ ) and collapsibility at the pterygoid hamulus showed a positive correlation with soft palate thickness ( $r=0.427$ ,  $P<0.05$ ).

The epiglottis was located below and above the soft palate in 13 and 10 dogs, respectively. In the analysis of differences in nasopharyngeal collapsibility according to epiglottis location, collapsibility at the caudal end of the soft palate was significantly larger when the epiglottis was located under the soft palate ( $P=0.026$ ).

In the analysis of the differences of nasopharyngeal area variants according to locations in each dog, there were significant

**Table 1.** Dimensions of the soft palate and their correlation with body weight in Beagle dogs (n=23)

Variable	Mean ± SD	Correlation coefficient with body weight
Soft palate length (mm)	64.51 ± 4.89	0.060 <sup>a</sup>
Soft palate thickness (mm)	6.48 ± 1.14	0.574 <sup>a, **</sup>

a, Pearson correlation coefficient; \*\*,  $P < 0.01$

**Table 2.** Maximum and minimum nasopharyngeal cross-sectional areas and its normalization at different locations in Beagle dogs (n=23)

Location	Nasopharyngeal CSA (mm <sup>2</sup> )		rCSAmax	rCSAmin
	Maximum	Minimum		
CrSP	0.98 ± 0.15	0.94 ± 2.29	1.02 ± 0.10	0.99 ± 0.10
PH	1.17 ± 0.33	1.12 ± 0.32	1.22 ± 0.32	1.17 ± 0.31
FL	1.25 ± 0.52	1.13 ± 0.50	1.31 ± 0.55	1.19 ± 0.53
BL	1.13 ± 0.45	1.02 ± 0.45	1.19 ± 0.50	1.07 ± 0.50
CdSP	1.03 ± 0.44	0.84 ± 0.43	1.09 ± 0.49	0.89 ± 0.46

The data presents the mean values ± standard deviation. CSA, cross-sectional area; rCSAmax, the ratio of maximum nasopharyngeal CSA to nasopharyngeal CSA at the level of the caudal hard palate; rCSAmin, the ratio of minimum nasopharyngeal CSA to nasopharyngeal CSA at the level of the caudal hard palate; CrSP, cranial end of the soft palate; PH, pterygoid hamulus; FL, foramen lacerum; BL, bony labyrinth; CdSP, caudal end of the soft palate.

**Table 3.** The nasopharyngeal collapsibility at each location and its correlation with body weight and dimension of the soft palate in Beagle dogs (n=23)

Location	Nasopharyngeal collapsibility (%)		Correlation coefficient		
	Median	1st / 3rd quartile	BW	SPL	SPT
CrSP	3.3	2.5 / 4.4	-0.073	-0.102	-0.208
PH	4.6	2.0 / 7.1	0.366	-0.347	0.427*
FL	9.2	5.3 / 12.4	0.112	-0.172	0.325
BL	10.2	6.0 / 13.4	0.499*	-0.162	0.393
CdSP	15.6	7.7 / 22.3	0.132	-0.445*	0.14

BW, body weight; SPL, soft palate length; SPT, soft palate thickness; CrSP, cranial end of the soft palate; PH, pterygoid hamulus; FL, foramen lacerum; BL, bony labyrinth; CdSP, caudal end of the soft palate; \* $P < 0.05$ .

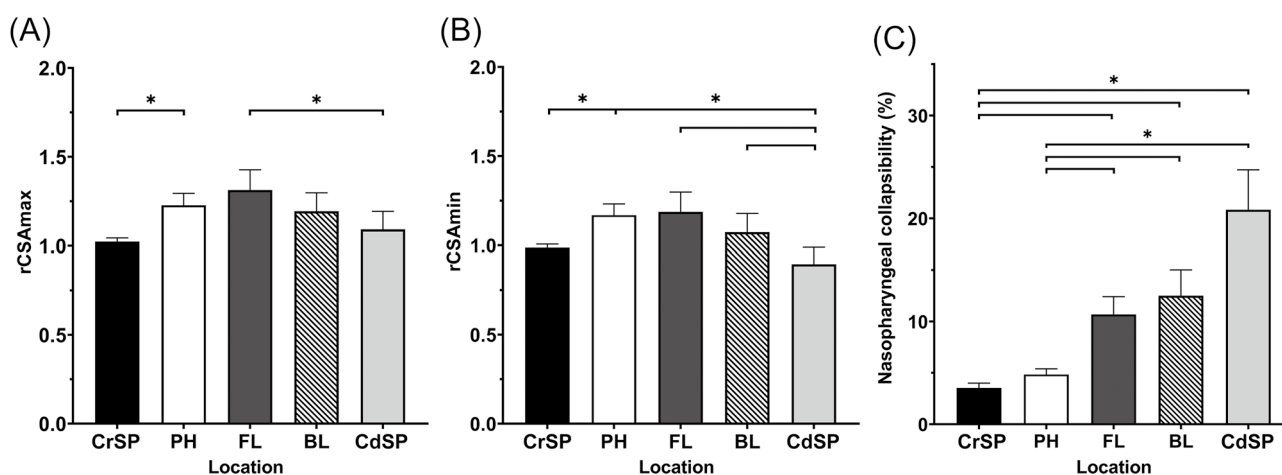


**Fig. 2.** Comparison of the nasopharyngeal area variants at the level of the cranial end of the soft palate (CrSP), pterygoid hamulus (PH), foramen lacerum (FL), bony labyrinth (BL), and the caudal end of the soft palate (CdSP) in Beagle dogs (n=23). All data is presented as the mean values with error bars (95% confidential intervals). The ratio of maximum cross-sectional area (rCSAmax) is significantly higher at the PH than that of CrSP, and rCSAmax at the level of FL is significantly higher than that of CdSP (A). rCSAmin at the level of PH is significantly higher than that of CrSP. rCSAmin at the level of CdSP is significantly lower than that of PH, FL, and BL (B). Nasopharyngeal collapsibility at CrSP and PH levels are significantly lower than those of FL, BL, and CdSP levels (C).  $P$ -values less than 0.05 are presented as \*.

differences in rCSAmax,  $F(2.01, 44.29) = 5.08, P < 0.05$ ; rCSAmin,  $F(1.86, 41.01) = 6.35, P < 0.01$ ; and nasopharyngeal collapsibility,  $F(1.83, 40.17) = 11.79, P < 0.01$ . The results of Bonferroni post hoc tests in nasopharyngeal area variants according to locations in each dog are presented in Fig. 2.

## DISCUSSION

In this study, nasopharyngeal CSA change during the respiratory cycle was detected and there was remarkable nasopharyngeal collapsibility at the level of foramen lacerum, bony labyrinth, and caudal part of the soft palate in normal Beagle dogs. These findings support the hypothesis that nasopharyngeal CSA change may exist even in normal dogs, and the degree of nasopharyngeal CSA change may differ depending on the location. Moreover, nasopharyngeal collapsibility has relationships with dimension of the soft palate and with epiglottis location.

There are several diagnostic imaging modalities to evaluate the anatomic or dynamic changes of the upper airway in dogs especially in brachycephalic breeds including radiography, rhinoscopy, fluoroscopy, static CT, and magnetic resonance imaging (MRI) [10, 12, 15, 16, 18, 21, 23, 24]. Among these modalities, fluoroscopy has been used in dogs with obstructive airway syndrome because it has the feasibility of real-time assessment of the dynamic profile of the upper airway and can be used without general anesthesia using an endotracheal tube [23, 24]. However, this has its limitation in that only 2-dimensional evaluation is possible. In humans, dynamic CT and MRI are used for evaluating dynamic changing of the upper airway in obstructive sleep apnea patients [9, 13]. Both modalities have the advantage of its feasibility of acquiring high-quality images and quantifying the dynamic profile. Considering that dogs need anesthesia for CT or MRI scans, MRI has the disadvantage as the anesthetic time is longer than that of CT. However, dynamic CT has several advantages including brief scan and anesthetic time and easy processing of imaging data for multiplanar reconstruction [9]. Therefore, dynamic CT was used in this study to evaluate dynamic profiles of the nasopharynx.

In this study, endotracheal intubation was not performed because it can induce artificial pressure given in the dogs [18]. During spontaneous inspiration with intubation, the negative airway pressure is generated by respiratory musculature to overcome the resistance of the endotracheal tube, aggravating the nasopharyngeal collapse in humans [8]. In brachycephalic dogs, changes of nasopharyngeal pressure may not appear because the endotracheal tube may act as a bypass, leading to reduced air flow through the nasopharynx [24]. Therefore, the results of the present study aim to reflect the natural pressure gradient during respiration, excluding artificial pressure factors. In addition, endotracheal intubation could affect the CSA of the caudal nasopharynx and soft palate length and it may preclude the evaluation of changing of nasopharyngeal dynamics [18, 24]. By not performing endotracheal intubation, this study could measure the nasopharyngeal CSA and soft palate length reflecting the same conditions as in the nature state.

In this study, we measured the angle between the hard palate and the dorsal margin of the vertebral canal to quantify the degree of head flexion. In a previous study on horses, pharyngeal diameter decreased with head flexion, which limited the airflow. This may result in turbulence followed by dynamic nasopharyngeal collapse [4]. Thus, the dog was positioned in an extended neutral position, enabling the avoidance of artificial nasopharyngeal collapse. The angle measured between head and cervical vertebrae was used to normalize the effect of head flexion in the nasopharyngeal area.

In humans, obstructive sleep apnea patients have a more collapsible velopharynx compared with normal subjects [6]. However, there has been no comparative study for nasopharyngeal collapsibility according to specific location in dogs with and without upper airway obstruction. In this study, various locations were selected to evaluate nasopharyngeal CSA and collapsibility at the level of the cranial end of the soft palate, pterygoid hamulus, foramen lacerum, bony labyrinth, and the caudal end of the soft palate. These anatomical levels for nasopharyngeal evaluation were chosen based on previous studies on brachycephalic dogs, and on their easiness to find that could be used in landmarks on CT [12, 15, 16, 25].

The level of the caudal end of the soft palate and foramen lacerum were considered suitable locations for detecting nasopharyngeal CSA change. The nasopharynx at the level of the caudal end of the soft palate showed lower rCSA<sub>min</sub> and higher collapsibility. This result is consistent with a previous study that showed the smallest nasopharyngeal CSA at the level of the caudal end of the soft palate in Pugs and French Bulldogs with obstructive airway syndrome [12]. These results may imply that the collapsibility at the caudal end of the soft palate may be high, regardless of symptoms or breed differences. This suggests that other levels of the nasopharynx may be needed to avoid overlapping of collapsibility when comparing dogs with and without obstructive airway syndrome. The nasopharynx at the foramen lacerum level was noteworthy as the rCSA<sub>max</sub> and rCSA<sub>min</sub> were higher than those of the caudal soft palate level and showed higher collapsibility than those of the cranial end of the soft palate and pterygoid hamulus in normal dogs. This may indicate that the nasopharynx at the foramen lacerum level could show differences in nasopharyngeal collapsibility with little overlap between normal dogs and dogs with clinical nasopharyngeal collapse. Further comparative studies of the nasopharynx using dynamic CT are needed in dogs with and without nasopharyngeal collapse.

In this study, positive correlations were found for nasopharyngeal collapsibility at the level of the pterygoid hamulus with soft palate thickness and nasopharyngeal collapsibility at the level of the bony labyrinth with body weight. These results are partially consistent with a previous study that revealed the soft palate thickness is the most relevant parameter in dogs with severe brachycephalic obstructive airway syndrome, whereas soft palate length is not [10]. In addition, weight gain can cause adipose tissue deposition on the soft palate, and obesity is a possible risk factor for development of pharyngeal collapse [22, 24]. These previous studies and result of present study suggest that either thickening of the soft palate or weight gain, or both, could affect nasopharyngeal collapsibility even in normal non-brachycephalic dogs.

In this study, dogs with the epiglottis located below the soft palate had higher nasopharyngeal collapsibility at the level of the caudal end of the soft palate. Epiglottis-overlying soft palate may cause the narrowing of the caudal nasopharyngeal area, resulting in high negative pressure. Similar to this condition, dorsal displacement of the soft palate in equines obstructs the normal airflow, resulting in more severe dynamic obstruction of the upper respiratory tract [5]. Moreover, the epiglottis may block the upward

movement of the soft palate when it is located above the soft palate, causing lower nasopharyngeal collapsibility. In this condition, the inspiration-induced negative pressure causing nasopharyngeal CSA change may be disturbed by the epiglottis blocking the upward movement of the soft palate. Anatomically, the natural location of the epiglottis at rest is dorsal to the soft palate, allowing nasal breathing. However, when breathing through the mouth, the epiglottis moves downward in mesocephalic dogs [2]. When a dog with respiratory distress presents open mouth breathing, nasopharyngeal collapsibility at the level of the caudal end of the soft palate may be higher in dogs with obstructive airway signs.

This study had some limitations. First, an anesthetic drug that may affect respiratory system was used because of the inevitable necessity of anesthesia for CT scans of dogs. However, respiratory depression of medetomidine alone is lower than other sedatives, even at sublethal doses [27]. Moreover, medetomidine is safe and widely used even in brachycephalic dogs with obstructive airway syndrome [7]. Second, the dynamic CT scan was performed at fixed scan intervals, and CT images at maximal inspiration and expiration may not have been obtained, which may be reflected in the calculated nasopharyngeal collapsibility. Third, Beagle dogs were used in this study and the result may differ from brachycephalic dogs, which have different upper airway conformation [22]. However, considering that nasopharyngeal collapse was also encountered in non-brachycephalic dog breeds [23, 24], the method described in this study would be applicable to non-brachycephalic dogs in small animal practice.

In conclusion, the findings from this study indicate that measurements of the nasopharyngeal collapsibility at the level of the caudal end of the soft palate and the foramen lacerum are considered useful locations. Either thickening of the soft palate, weight gain, or epiglottis location could affect the nasopharyngeal collapsibility even in normal Beagle dogs. Dynamic CT could show the dynamic profile of the airway and would be an adequate modality for evaluating the nasopharynx in dogs. Further dynamic CT study of the nasopharynx is needed to compare the collapsibility in dogs with and without obstructive airway syndrome.

**CONFLICT OF INTEREST.** None of the authors have a financial or personal relationship with other people or organizations that could inappropriately influence or bias the content of the paper.

## REFERENCES

1. Ayappa, I. and Rapoport, D. M. 2003. The upper airway in sleep: physiology of the pharynx. *Sleep Med. Rev.* **7**: 9–33. [Medline] [CrossRef]
2. Baker, G. J. 1972. Surgery of the canine pharynx and larynx. *J. Small Anim. Pract.* **13**: 505–513. [Medline] [CrossRef]
3. Campana, L., Eckert, D. J., Patel, S. R. and Malhotra, A. 2010. Pathophysiology & genetics of obstructive sleep apnoea. *Indian J. Med. Res.* **131**: 176–187. [Medline]
4. Cehak, A., Rohn, K., Barton, A. K., Stadler, P. and Ohnesorge, B. 2010. Effect of head and neck position on pharyngeal diameter in horses. *Vet. Radiol. Ultrasound* **51**: 491–497. [Medline] [CrossRef]
5. Chesen, A. B. and Whitfield-Cargile, C. 2015. Update on diseases and treatment of the pharynx. *Vet. Clin. North Am. Equine Pract.* **31**: 1–11. [Medline] [CrossRef]
6. Ciscar, M. A., Juan, G., Martínez, V., Ramón, M., Lloret, T., Mínguez, J., Armengot, M., Marín, J. and Basterra, J. 2001. Magnetic resonance imaging of the pharynx in OSA patients and healthy subjects. *Eur. Respir. J.* **17**: 79–86. [Medline] [CrossRef]
7. Downing, F. and Gibson, S. 2018. Anaesthesia of brachycephalic dogs. *J. Small Anim. Pract.* **59**: 725–733. [Medline] [CrossRef]
8. Fiastro, J. F., Habib, M. P. and Quan, S. F. 1988. Pressure support compensation for inspiratory work due to endotracheal tubes and demand continuous positive airway pressure. *Chest* **93**: 499–505. [Medline] [CrossRef]
9. Fleck, R. J., Ishman, S. L., Shott, S. R., Gutmark, E. J., McConnell, K. B., Mahmoud, M., Mylavarapu, G., Subramaniam, D. R., Szczesniak, R. and Amin, R. S. 2017. Dynamic volume computed tomography imaging of the upper airway in obstructive sleep apnea. *J. Clin. Sleep Med.* **13**: 189–196. [Medline] [CrossRef]
10. Grand, J. G. R. and Bureau, S. 2011. Structural characteristics of the soft palate and meatus nasopharyngeus in brachycephalic and non-brachycephalic dogs analysed by CT. *J. Small Anim. Pract.* **52**: 232–239. [Medline] [CrossRef]
11. Hara, Y., Teshima, K., Seki, M., Asano, K. and Yamaya, Y. 2020. Pharyngeal contraction secondary to its collapse in dogs with brachycephalic airway syndrome. *J. Vet. Med. Sci.* **82**: 64–67. [Medline] [CrossRef]
12. Heidenreich, D., Gradner, G., Kneissl, S. and Dupré, G. 2016. Nasopharyngeal dimensions from computed tomography of Pugs and French bulldogs with brachycephalic airway syndrome. *Vet. Surg.* **45**: 83–90. [Medline] [CrossRef]
13. Huon, L. K., Liu, S. Y. C., Shih, T. T. F., Chen, Y. J., Lo, M. T. and Wang, P. C. 2016. Dynamic upper airway collapse observed from sleep MRI: BMI-matched severe and mild OSA patients. *Eur. Arch. Otorhinolaryngol.* **273**: 4021–4026. [Medline] [CrossRef]
14. Isono, S., Remmers, J. E., Tanaka, A., Sho, Y., Sato, J. and Nishino, T. 1997. Anatomy of pharynx in patients with obstructive sleep apnea and in normal subjects. *J Appl Physiol (1985)* **82**: 1319–1326. [Medline] [CrossRef]
15. Jones, B. A., Stanley, B. J. and Nelson, N. C. 2020. The impact of tongue dimension on air volume in brachycephalic dogs. *Vet. Surg.* **49**: 512–520. [Medline] [CrossRef]
16. Kim, Y. J., Lee, N., Yu, J., Lee, H., An, G., Bang, S., Chang, J. and Chang, D. 2019. Three-dimensional volumetric magnetic resonance imaging (MRI) analysis of the soft palate and nasopharynx in brachycephalic and non-brachycephalic dog breeds. *J. Vet. Med. Sci.* **81**: 113–119. [Medline] [CrossRef]
17. Laurenson, M. P., Zwingerberger, A. L., Cissell, D. D., Johnson, L. R., McPeters, M. J., Spriet, M. P., Taylor, S. L. and Pollard, R. E. 2011. Computed tomography of the pharynx in a closed vs. open mouth position. *Vet. Radiol. Ultrasound* **52**: 357–361. [Medline] [CrossRef]
18. Liu, N. C., Troconis, E. L., McMillan, M., Genain, M. A., Kalmar, L., Price, D. J., Sargan, D. R. and Ladlow, J. F. 2018. Endotracheal tube placement during computed tomography of brachycephalic dogs alters upper airway dimensional measurements. *Vet. Radiol. Ultrasound* **59**: 289–304. [Medline] [CrossRef]
19. Malhotra, A., Pillar, G., Fogel, R., Beauregard, J., Edwards, J. and White, D. P. 2001. Upper-airway collapsibility: measurements and sleep effects. *Chest* **120**: 156–161. [Medline] [CrossRef]
20. Malhotra, A., Huang, Y., Fogel, R., Lasic, S., Pillar, G., Jakab, M., Kikinis, R. and White, D. P. 2006. Aging influences on pharyngeal anatomy and physiology: the predisposition to pharyngeal collapse. *Am. J. Med.* **119**: 72.e9–72.e14. [Medline] [CrossRef]

21. Noone, K. E. 2001. Rhinoscopy, pharyngoscopy, and laryngoscopy. *Vet. Clin. North Am. Small Anim. Pract.* **31**: 671–689. [[Medline](#)] [[CrossRef](#)]
22. Packer, R. M. A., Hendricks, A., Tivers, M. S. and Burn, C. C. 2015. Impact of facial conformation on canine health: brachycephalic obstructive airway syndrome. *PLoS One* **10**: e0137496. [[Medline](#)] [[CrossRef](#)]
23. Pollard, R. E., Johnson, L. R. and Marks, S. L. 2018. The prevalence of dynamic pharyngeal collapse is high in brachycephalic dogs undergoing videofluoroscopy. *Vet. Radiol. Ultrasound* **59**: 529–534. [[Medline](#)] [[CrossRef](#)]
24. Rubin, J. A., Holt, D. E., Reetz, J. A. and Clarke, D. L. 2015. Signalment, clinical presentation, concurrent diseases, and diagnostic findings in 28 dogs with dynamic pharyngeal collapse (2008–2013). *J. Vet. Intern. Med.* **29**: 815–821. [[Medline](#)] [[CrossRef](#)]
25. Sarran, D., Caron, A., Testault, I., Segond, S. and Billet, J. P. 2018. Position of maximal nasopharyngeal maximal occlusion in relation to hamuli pterygoidei: use of hamuli pterygoidei as landmarks for palatoplasty in brachycephalic airway obstruction syndrome surgical treatment. *J. Small Anim. Pract.* **59**: 625–633. [[Medline](#)]
26. Schwab, R. J., Geffer, W. B., Pack, A. I. and Hoffman, E. A. 1993. Dynamic imaging of the upper airway during respiration in normal subjects. *J Appl. Physiol. (1985)* **74**: 1504–1514. [[Medline](#)] [[CrossRef](#)]
27. Sinclair, M. D. 2003. A review of the physiological effects of  $\alpha 2$ -agonists related to the clinical use of medetomidine in small animal practice. *Can. Vet. J.* **44**: 885–897. [[Medline](#)]
28. Yucel, A., Unlu, M., Haktanir, A., Acar, M. and Fidan, F. 2005. Evaluation of the upper airway cross-sectional area changes in different degrees of severity of obstructive sleep apnea syndrome: cephalometric and dynamic CT study. *AJNR Am. J. Neuroradiol.* **26**: 2624–2629. [[Medline](#)]